The LHC Diphoton excess at 750 GeV in the framework of the Constrained Minimal Supersymmetric Standard Model

Debajyoti Choudhury[1] and Kirtiman Ghosh[2]
Department of Physics and Astrophysics, University of Delhi, Delhi 110007, India
[1] *debajyoti.choudhury@gmail.com,* [2] *kirti.gh@gmail.com*

We examine the observed diphoton excess at 750 GeV in the framework of constrained Minimal Supersymmetric Standard Model (cMSSM). The consistency of cMSSM with the discovery of a 125 GeV Higgs boson and PLANCK/WMAP data for dark matter relic density (RD) demands large mixing in the scalar top (stop) sector and consequently, the existence of a light stop quasi-degenerate with the lightest neutralino. Small decay width due to kinematic and loop suppression of such a stop allows for the existence of stop-antistop bound states (stoponia). Identifying the particular part of cMSSM parameter space consistent with Higgs boson mass as well as RD, we study stoponia as the source of the diphoton excess.

arXiv:1605.00013v2 [hep-ph] 30 May 2016

Recent LHC reports [1, 2] of a diphoton excess at about 750 GeV invariant mass could be interpreted as production and decay of a new massive spin-0 or spin-2 particle. The ATLAS collaboration observed the most significant deviation from the background predictions at $M_{\gamma\gamma} \sim$750 GeV with a local significance of 3.6σ and 3.9σ in searches optimized for a spin-2 and spin-0 particle, respectively. For the CMS collaboration, the largest excess is observed around $M_{\gamma\gamma} \sim 760$ GeV with corresponding local significance of 2.8σ (2.9σ). Under the narrow width approximation, the fitted LHC 13 TeV ATLAS and CMS data correspond to a resonance with effective signal strength (namely, production cross-section times branching ratio into $\gamma\gamma$) of 10 ± 3 and $2 \sim 6$ fb, respectively. The best fitted values for the decay width are 45 GeV for the ATLAS data and 0.1 GeV for CMS Run I and II data combined. This large discrepancy is perhaps reflective of the limited statistics and we shall return to this issue later.

The excess has motivated many phenomenological studies [3, 4] of possible scenarios of new physics beyond the SM. The mutual consistency of the LHC 8 TeV (no diphoton signature) [5, 6] and 13 TeV (diphoton excess) results demands that gluon-gluon fusion be the dominant mechanism for the production of the resonance. Adopting the spin-0 hypothesis[1], the (pseudo)scalar couples with a pair of gluons/photons only at the loop level. To explain the signal size and profile, one needs to postulate additional (and heavy enough not to have been seen) colored and charged states with large couplings to the resonance so as to enhance its induced coupling to a pair of gluons/photons. On the other hand, if the resonance is a QCD bound-state of new colored (charged) particles then it automatically couples to a pair of gluons (photons) via the annihilation Feynman diagram. Resonant production of particle-antiparticle ($X\bar{X}$) bound-state (η_X) at collider is possible if the formation time ($\sim$ the inverse of binding energy, E_b) of η_X is smaller than the life-time ($\sim$ inverse of decay width, Γ_X) of X: $\Gamma_X \ll E_b$. Subsequently, the decay of the η_X may proceed either through the prompt decay of the constituent X or through annihilation diagrams. If the annihilation decay width (Γ_{η_X}) dominates over Γ_X, we could, potentially, observe the resonant signature η_X at colliders before discovering the new particle X. Historically, the first signals for c– and b-quarks in hadron colliders were leptonic decays of their $J/\psi(\bar{c}c)$ or $\Upsilon(\bar{b}b)$ bound states. Therefore, if there is a colored particle in nature with few hundred GeV mass and suppressed decay, then the signature of the bound state could pop up before the discovery of the particle itself. As a result, there is a fair amount of effort going on to explain the 750 GeV diphoton resonance as a QCD bound state [8]. In this work, we explain the diphoton excess in the framework of supersymmetry (SUSY), which predicts the existence of TeV scale colored fermions (partners of gluons namely, gluinos) and scalars (partners of the SM quarks namely, squarks). To retain a viable dark matter (DM) candidate, we will impose R-parity conservation. Consequently, if the tree-level 2-body decay of a colored SUSY-particle into a lighter SUSY-particle is kinematically (or otherwise) suppressed, then its individual decay width could be small enough to give rise to a bound-state, albeit short-lived. In particular, if the mass splitting between the of top-squark (the stop) and the lightest neutralino $\tilde{\chi}_1^0$ (the lightest supersymmetric particle or LSP) is small enough to forbid the 2-body decay of stop into $t\tilde{\chi}_1^0$ (or a bottom-chargino pair), then a stop-antistop bound pair (stoponium) is a distinct possibility [9–11] We explore this, restricting ourselves to the framework of the constrained Minimal Supersymmetric Standard Model (cMSSM).

Apart from usual motivations like stability of the Higgs mass, an explanation for dark matter etc., the cMSSM has the advantage of having a mathematically well constructed mechanism for supersymmetry breaking at GUT scale. With the phenomenology determined by only four parameters at GUT scale namely, common SUSY breaking scalar (m_0) and gaugino ($m_{1/2}$) masses, a single tri-

[1] While a Randall-Sundrum-type graviton has been offered as a solution, suppressing the decay into a $t\bar{t}$ or a dilepton pair (none of which has been seen), is not very straightforward [7].

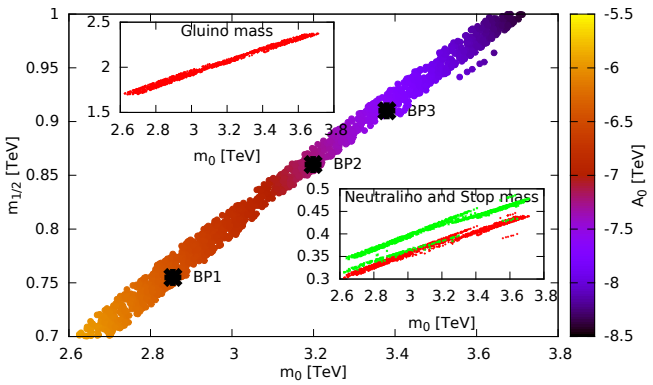

FIG. 1. The 3-dimensional parameter space consistent with Higgs discovery and RD data, for $\tan\beta = 15$ and $\mu > 0$. The inset figures corresponds to scatter plots for LSP, lightest stop (bottom) and gluino (top) mass.

linear mass parameter A_0, ratio of Higgs vacuum expectation values $\tan\beta$ and the discrete choice of the sign of the Higgs mixing parameter μ, the model is highly predictive and easy to probe in collider experiments. At the LHC, production of squarks and gluinos play the most important roles in discovering cMSSM, with perhaps the best signature being the multi-jets plus missing transverse energy ($\not{E}_T$) channel where $\not{E}_T$ results from the weakly interacting LSPs appearing in the final state. However, at the LHC RUN I and RUN II [12, 13], no such signature has been detected and thus, equal squark and gluino masses below 1.85 TeV are excluded at 95% confidence level (C.L.). These lower bounds do not militate against the mechanism for stabilizing the electroweak hierarchy from large radiative corrections, as only the third generation squarks are important at one loop order and LHC searches are not yet very sensitive for these. Indeed, a stop mass of a few hundred GeVs is still allowed and, in fact, favored by fine-tuning arguments. Within the framework of cMSSM, a light stop can naturally arises as a consequence of large third-generation Yukawa coupling. With the off-diagonal terms in the mass matrix for the squark of a given flavor being proportional to the Yukawa coupling and growing with A_0, a large A_0 can generate a large mass splitting in the stop sector and consequently produce a light stop ($\tilde{t}_1$) as the next-to-lightest supersymmetric particle (NLSP).

In fact, a quasi-degenerate $\tilde{t}_1$-NLSP is inherent to the only part of the cMSSM parameter space which simultaneously explains WMAP/PLANCK [14, 15] DM relic density (RD) data as well as the LHC discovery of a 126 GeV Higgs boson. Most of the cMSSM parameter space gives rise to a bino-like LSP and, hence, too large a RD. For a quasi-degenerate $\tilde{t}_1$-$\tilde{\chi}_1^0$ pair, though, the observed relic density can be explained via $\tilde{t}_1$-$\tilde{\chi}_1^0$ coannihilation. Furthermore, electroweak (EW) baryogenesis favors a light-$\tilde{t}_1$ [16]. Interestingly, this very same part

TABLE I. Benchmark parameters and relevant sparticle masses in GeV ($\tan\beta = 15$, $\mu > 0$).

BPs	m_0	$m_{1/2}$	A_0	$m_{\tilde{g}}$	$m_{\tilde{t}_2}$	$m_{\tilde{t}_1}$	$m_{\tilde{\chi}_1^\pm}$	$m_{\tilde{\chi}_1^0}$	m_h
BP1	2855	755	-6467	1821	2213	370	643	334	127.3
BP2	3199	860	-7277	2052	2480	420	734	383	126.3
BP3	3380	910	-7695	2162	2616	445	777	406	127.5

of the cMSSM parameter space is also suitable for the production of stoponia at the LHC, and we now carefully examine it.

With the off-diagonal term being given by $M_{LR}^2 = m_t(A_t - \mu\cot\beta)$, the mass splitting is maximized when μ and A_t have opposite signs. Choosing $\mu > 0$ and a representative value of $\tan\beta = 15$, we scan over m_0, $m_{1/2}$ and A_0 to obtain the phenomenologically acceptable part of the parameter space. The particle spectrum was calculated using **SuSpect** [17] with $m_t = 173.2$ GeV, $m_b = 4.2$ GeV, $m_\tau = 1.777$ GeV and $\alpha_s(m_Z) = 0.1172$. Fig. 1 shows a 3-dimensional scatter plot, in the m_0-$m_{1/2}$ plane with A_0 being indicated by color gradient, of the parameter space consistent with the Higgs mass 126 ± 2 GeV and WMAP/PLANCK RD data. The density of cold dark matter in the universe is determined to be [14] $\Omega_c h^2 = 0.1186 \pm 0.0036$. However, we only demand that the RD due to $\tilde{\chi}_1^0$ (which we calculate using **micrOmegas** [18]) does not exceed the bound at the 2σ level. Furthermore, to account for the higher order effects in RD calculations and the consequent small inaccuracies in **micrOmegas** [19], we relax the bound to $\Omega_c h^2 < 0.1311$. Fig. 1 shows that there is only a narrow region in the cMSSM parameter space consistent with both Higgs mass and RD data. The situation is very similar for other values of $\tan\beta$. In the insets of Fig. 1, we present the resulting $\tilde{\chi}_1^0$, $\tilde{t}_1$ (bottom) and $\tilde{g}$ (top) masses. In particular, note the small mass splitting between the first two.

It is also important to check the consistency of the model with other constraints like $BR(B \to X_s\gamma) = (355 \pm 142) \times 10^{-6}$ [20], $BR(B_s \to \mu^+\mu^-) < 4.5 \times 10^{-9}$ (95% C.L.) [21], $0.99 < R_{\tau\nu_\tau}^{NP} = \frac{BR(B^+\to\tau^+\nu_\tau)_{SM+NP}}{BR(B^+\to\tau^+\nu_\tau)_{SM}} < 3.19$ [22] as well as direct collider searches at the LHC RUN I and II. To illustrate further numerical results, we choose three benchmark points (BP), indicated by black dots in Fig. 1 and listed in Table I, along with the masses of the relevant sparticles and the light Higgs boson. For the parameter-space in Fig. 1, the other squarks are heavier than the $\tilde{g}$ and, hence, $\tilde{\chi}_1^0$, $\tilde{t}_1$ and $\tilde{g}$ are the most important particles in the context of LHC searches. In Table II, we also list the next-to-leading (NLO) order production cross-sections for $\tilde{t}_1\tilde{t}_1^*$ and $\tilde{g}\tilde{g}$ pairs at the LHC with 8 and 13 TeV center-of-mass energy, as calculated using **Prospino** 2.1 [23] with CTEQ6.6M [24] parton distribution functions. Inspite of the substantial production cross-section, $\tilde{t}_1$-signatures are hard to detect because of the small $m_{\tilde{t}_1}$-$m_{\tilde{\chi}_1^0}$ splitting. The kinematically allowed

TABLE II. Low energy constraints, light stop decay width and NLO $\tilde{t}_1 x t^*$, $\tilde{g}\tilde{g}$ production cross-section at the LHC 8 and 13 TeV.

BPs	$\mathrm{BR}^B_{X_s\gamma}$ $\times 10^4$	$\mathrm{BR}^{B_s}_{\mu\mu}$ $\times 10^9$	$R^{NP}_{\tau\nu_\tau}$	$\Omega_c h^2$ eV	$\sigma(\tilde{t}_1\tilde{t}_1^*)$ [pb] 8	13	$\sigma(\tilde{g}\tilde{g})$ [fb] 8	13
BP1	3.10	3.12	0.99	0.116	0.55	2.64	0.016	1.55
BP2	3.14	3.11	0.99	0.122	0.25	1.32	0.002	0.45
BP3	3.15	3.11	0.99	0.128	0.18	0.96	0.001	0.26

$\tilde{t}_1$ decays namely, loop induced flavor violating 2-body decay into $c\tilde{\chi}^0_1$ and tree-level four body decay into a b-quark in association with pair of light quarks and $\tilde{\chi}^0_1$, give rise to very soft jets and $\not{p}_T$ signature which is very hard to detect over the huge SM backgrounds. Several alternative signatures like stop pair production in association with two b-jets [25], single photon [26] or jet [27], have been proposed in the literature. Mono-jet or a charm-jet+$\not{p}_T$ search at the LHC with $\sqrt{s} = 8$ TeV and $\mathcal{L} = 20.3$ fb^{-1} puts a lower bound of 270 GeV [28] on $\tilde{t}_1$-mass for a degenerate $m_{\tilde{t}_1}$-$m_{\tilde{\chi}^0_1}$ scenario. As for $\tilde{g}\tilde{g}$-production, since the gluino overwhelmingly decays into a top-stop pair, the signature would be pair of tops accompanied by some very soft jets and $\not{p}_T$. For $\sqrt{s} = 8$ TeV, the ATLAS [29] collaboration studied an analogous process, namely stop-pair production with the stop decaying promptly into $t\tilde{\chi}^0_1$-pairs. The negative result can be roughly translated to a model independent upper bound of 13.9 fb on the BSM contribution to $t\bar{t} + \not{p}_T$. Table II shows that the gluino-pair production cross-sections are much smaller than this bound. Therefore, the BPs as well as the parameter space are completely consistent with all the constraints.

A stoponium can form only if its binding energy is greater than the stop decay width. In the present case, apart from the phase space suppression, the 2-body decay $\tilde{t}_1 \to c\tilde{\chi}^0_1$ is also suppressed by the loop as well as flavor violation factors, whereas the 4-body decay $\tilde{t}_1 \to bq\bar{q}'\tilde{\chi}^0_1$ is suppressed due to the heavy particles in the propagators. $\tilde{t}_1$ decay widths for BP1, BP2 and BP3 are estimated (using SUSY-HIT1.5 [30]) to be 1.28×10^{-10}, 9.96×10^{-10} and 9.03×10^{-10} GeV respectively. On the other hand, the typical binding energy of a QCD bound-state is $E_b \sim \alpha_s m_{\tilde{t}_1}/a_0^2 \sim \mathcal{O}(\mathrm{GeV})$ where a_0 is the Bohr radius of the system. Thus, stoponia may indeed exist. Once the bound-state is formed, it can decay either via annihilation of its constituents to boson/fermion pairs or via the decay of the constituents themselves. Only the former would give rise to a distinctive resonance signature. The annihilation partial decay widths of the $1S$ state into a pair of gluons and photons are given by,

$$\Gamma^{gg}_{\eta_{\tilde{t}_1}} = \frac{4}{3}\,\alpha_S^2\,\Delta \qquad \text{and} \qquad \Gamma^{\gamma\gamma}_{\eta_{\tilde{t}_1}} = \frac{32}{27}\,\alpha^2\,\Delta\ , \qquad (1)$$

where Δ is a parameter with a dimension of mass and, for a non-relativistic (i.e., binding energy much smaller than the constituent mass) bound-state, Δ is given in terms of the radial wavefunction at the origin $\psi(0) = \sqrt{4\pi}R(0)$, viz. $\Delta = |R(0)|^2/m^2_{\eta_{\tilde{t}_1}}$. In Ref. [31], $|R(0)|$, and the binding energy of a non-relativistic bound state was computed in the framework of potential models. Using $\Lambda^{(4)}_{\overline{MS}} = 300$ MeV and the parametrization of Ref [31], the non-relativistic stoponium binding energy (namely, $2m_{\tilde{t}_1} - m_{\eta_{\tilde{t}_1}} \sim 3.274 + 1.777L + 0.560L^2 + 0.081L^3$ GeV where $L = \ln(m_{\tilde{t}_1}/250\mathrm{GeV})$) and stoponium mass for BP1 are estimated to be 4.1 GeV and 736 GeV, respectively. Thus, BP1 could potentially explain the diphoton excess provided the stoponium production cross-section and decay to $\gamma\gamma$ are consistent with the observed excess.

A recent study of the stoponium [32] using the lattice formulation of nonrelativistic effective field theory (NREFT), yields $\Delta \sim 0.57$ GeV for the 750 GeV 1S state, which is a factor of 3.5–4 larger than that obtained within naive potential models. The consequent partial decay width of such as state into a pair of gluons (photons) can be estimated to be 7.5×10^{-3} (4.2×10^{-5}) GeV. With the bound state decaying much faster than the constituents themselves, a resonant structure to the signal, thus, follows.

Stoponium production cross-section at the LHC resulting from gluon-gluon fusion can be obtained by convoluting $\Gamma^{gg}_{\eta_{\tilde{t}_1}}$ with the gluon densities, $g(x, Q^2)$, in the colliding protons:

$$\sigma^{pp}_{\eta_{\tilde{t}_1}} = \frac{\pi^2}{8m^3_{\eta_{\tilde{t}_1}}}\Gamma^{gg}_{\eta_{\tilde{t}_1}} \int_\tau^1 dx \frac{\tau}{x} g\left(x, Q^2\right) g\left(\frac{\tau}{x}, Q^2\right), \qquad (2)$$

where $\tau = m^2_{\eta_{\tilde{t}_1}}/s$. Using the aforementioned widths, and assuming that no other decay mode exists, the diphoton cross section for $\sqrt{s} = 13$ TeV, is approximately 0.19 fb. In other words, within the the NREFT framework, the cross-section is nearly one order of magnitude smaller than the observed excess. A few enhancements are operative, though. For one, the NLO QCD correction [11] leads to a K-factor of approximately 1.38. Moreover, the 1S state is not the only one that is present or can be produced. For all the nS states, the formalism is identical. However, with $R(0)$ being smaller, the individual production rates would be progressively smaller. And while their partial widths into the exclusive $\gamma\gamma$ mode are smaller, it is not so for the branching fraction, especially where the semi-inclusive rate (alongwith soft radiations) is concerned. As for the P-wave states, understandably, they cannot be formed directly from gg fusion. However, the radiation of a soft gluon clearly allows this, much like the case of J/ψ or the Υ. However, even on the inclusion of all such effects, the overall enhancement is not expected to be larger than about 2.5. Thus, the observed rates cannot still be explained in totality. More interestingly though, the large width observed by ATLAS could be partially explained owing to the spread in the masses of the bound states.

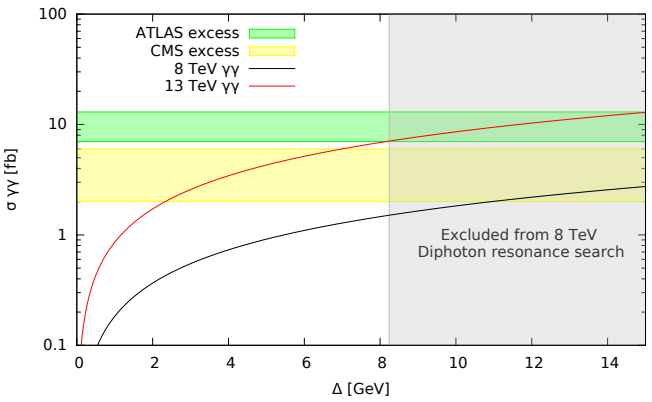

FIG. 2. Production cross-section of a 750 GeV relativistic stoponium decaying into diphoton as a function of Δ at the LHC with 8 and 13 TeV center-of-mass energy. Yellow and green shaded regions indicate the fitted ranges for the diphoton excess at the CMS and ATLAS respectively.

The large coupling $A_t H_u \tilde{Q}_L \tilde{t}_R$ provides another attractive force between stop-antistop pairs mediated by the exchange of the scalar quanta. Analytically solving a Bethe-Salpeter equation for the bound state in the framework of the Wick-Cutkosky model [33] for massless scalar exchange, Ref. [34] predicted the existence of two-stop composite states with binding energies of the order of the electroweak scale for large $A_t (\sim$ few TeV) and small $m_{\tilde{t}_1} (\sim$ few hundred GeV). The Wick-Cutkosky model for a massive exchange scalar was studied in Ref. [35] and the existence of relativistic bound-states was predicted for large enough coupling. There are several interesting consequences of such a relativistic bound state. For example, the stoponium could develop a non-zero VEV and contribute to electroweak breaking [34]. Mixing of the stoponium with the Higgs could not only generate EW-symmetry breaking from supersymmetry breaking [36, 37], but also enhance the Higgs mass[2]. The critical value of A_t, required for symmetry-breaking seesaw to occur, was estimated to be of the order of a few TeVs.

With the mass of a relativistic bound-state not being well-understood in terms of the constituent mass (except for the fact that the binding energy is relatively large), BP2 and BP3 are representative points in the parameter space. Similarly, $\Delta = |R(0)|^2/m^2_{\eta_{\tilde{t}_1}}$ is no longer applicable and Δ has to be treated as an unknown parameter which is expected to be much larger. As Fig. 2 shows, the diphoton excess can be explained by relativistic stoponium production for 2.32 GeV $< \Delta <$ 8.24 GeV. Once again, we have neglected both NLO corrections as well as contributions from the excited stoponia. Inclusion of these would move the Δ-window to slightly lower values, while broadening the observed width.

Some issues remain. We have, until now, neglected branching modes other than than gg and $\gamma\gamma$. However, as Ref.[10] shows, for a non-relativistic stoponium, $\Gamma_{X\bar{X}}$ $(X = W, Z, h, t)$ and $\Gamma_{\gamma\gamma}$ are orders of magnitude smaller than Γ_{gg}. Thus, $Br(\eta_{\tilde{t}_1} \to \gamma\gamma)$ remains essentially unchanged. Moreover, once branching fractions for the cascades are included, the $X\bar{X}$ channels would remain undetectable. And, of course, the dilepton channel is even more suppressed. What remains irreconciled, though, is the large width reported by ATLAS (in contrast to CMS). Even accounting for detector effects and a low statistics, such a large width can only be accommodated if the stoponium were to have a very large decay width into (quasi-)invisible channels, much larger than $\Gamma_{\tilde{\chi}^0_1\tilde{\chi}^0_1}$ (if kinematically allowed) is.

And, finally, we come to confirmatory tests for our hypothesis. Obvious candidates are $\tilde{t}_1\tilde{t}_1^*$ production [39] in association with a light object, such as a γ, Z, a jet, or given the large A_t, even h. As already discussed, the strongest present bound for degenerate $\tilde{t}_1$-$\tilde{\chi}^0_1$ scenario comes from $\tilde{t}_1\tilde{t}_1^*$+jets analysis and with more luminosity, other channels become increasingly feasible. The characteristic feature of cMSSM with degenerate $\tilde{t}_1$-$\tilde{\chi}^0_1$ is the existence of a heavy ($\sim 5m_{\tilde{t}_1}$, see Fig. 1) gluino decaying into top-stop $(t\tilde{t}_1^* + \bar{t}\tilde{t}_1)$ pairs with 100% BR. Therefore, $\tilde{g}\tilde{g}$-pair production (although highly suppressed, see Table II) gives rise to confirmatory signatures namely, 2-boosted top-jets+large $\not{p}_T$(because of large $m_{\tilde{g}} - m_{xt}$ splitting) [42], same-sign top-pairs+large $\not{p}_T$ (when both gluino decays into $t\tilde{t}_1^*$- or $\bar{t}\tilde{t}_1$-pairs) [38] e.t.c., for our hypothesis. Assuming 80% efficiency (ϵ) [40] for tagging hadronically decaying boosted ($p_T^{(\rm top)} > 300$ GeV) top at 13 TeV LHC, naive estimation of $\sigma(\tilde{g}\tilde{g}) \times \text{Br} \times \epsilon$ (see Table II) yields 45, 13 and 7 two high-p_T top-jets + large $\not{p}_T$ events for BP1, BP2 and BP3, respectively, for $\mathcal{L} = 100$ fb^{-1}. Therefore, probing boosted-tops signature of BP1, BP2 and BP3 is possible with suitable cuts (large p_T-cuts for top-jets and missing-p_T) to kill the SM background completely without affecting the signal [42]. Same-sign ditop signature of our hypothesis is particularly intriguing in view of the reported excess of same-sign dilepton (SSD) plus $b\bar{b}$ events at the LHC Run I [43]. The large $\tilde{g}$-mass and thus, small $\sigma(\tilde{g}\tilde{g})$ for the our BPs can not explain the reported excess. However, were we deviate from the usual cMSSM by incorporating non-universal boundary conditions for the gaugino masses (as happens, for example, for non-trivial gauge kinetic functions in the supergravity framework), the gluino can be substantially lighter leading to a SSD+$b\bar{b}$ excess as reported by ATLAS [43]. And, finally, at a future e^+e^-

[2] Such considerations also save the scenario from potential constraints from color-breaking minima that a large A_0 often entails. With the inclusion of the bound states now being mandatory, the nominal one-loop corrected scalar potential [41] involving only sfermions and Higgses does not hold any longer and the phase-diagram needs to be redetermined. While this also has a bearing on Fig.1, there is no qualitative change.

linear collider, a threshold scan would show up several of the stoponia, in particular the nP-states.

DC acknowledges partial support from the European Union's Horizon 2020 research and innovation programme under Marie Sklodowska-Curie grant No 674896, and the R&D grant of the University of Delhi. KG is supported by DST (India) under INSPIRE Faculty Award.

[1] The ATLAS collaboration, ATLAS-CONF-2015-081; ATLAS-CONF-2016-018.

[2] CMS Collaboration, CMS-PAS-EXO-16-018; CMS-PAS-EXO-15-004.

[3] J. Ellis *et. al.*, JHEP **1603**, 176 (2016).

[4] B.C. Allanach *et al.*, arXiv:1512.07645 [hep-ph]; F. Wang *et al.*, arXiv:1512.06715 [hep-ph]; R. Ding *et al.*, arXiv:1512.06560 [hep-ph]; T. F. Feng *et al.*, arXiv:1512.06696 [hep-ph]; L. M. Carpenter, R. Colburn and J. Goodman, arXiv:1512.06107 [hep-ph]; H. P. Nilles and M. W. Winkler, arXiv:1604.03598 [hep-ph]; R. Barbieri *et al.*, arXiv:1603.00718 [hep-ph]; U. Ellwanger and C. Hugonie, arXiv:1602.03344 [hep-ph]; S. F. King and R. Nevzorov, JHEP **1603**, 139 (2016); B. Dutta *et al.*, arXiv:1601.00866 [hep-ph]; W. Chao, arXiv:1601.00633 [hep-ph]; F. Wang *et al.*, arXiv:1512.08434 [hep-ph]. L. J. Hall, K. Harigaya and Y. Nomura, JHEP **1603**, 017 (2016); J. A. Casas, J. R. Espinosa and J. M. Moreno, arXiv:1512.07895 [hep-ph]; M. Badziak, M. Olechowski, S. Pokorski and K. Sakurai, arXiv:1603.02203 [hep-ph]; F. Domingo, S. Heinemeyer, J. S. Kim and K. Rolbiecki, arXiv:1602.07691 [hep-ph]; U. Ellwanger and C. Hugonie, arXiv:1602.03344 [hep-ph]. P. Baratella, J. Elias-Miro, J. Penedo and A. Romanino, arXiv:1603.05682 [hep-ph]; D. Bardhan, P. Byakti, D. Ghosh and T. Sharma, arXiv:1603.05251 [hep-ph]; J. J. Heckman, Nucl. Phys. B **906**, 231 (2016); X. F. Han and L. Wang, Phys. Rev. D **93**, no. 5, 055027 (2016); S. Di Chiara, L. Marzola and M. Raidal, Phys. Rev. D **93**, no. 9, 095018 (2016).

[5] G. Aad *et al.* [ATLAS Collaboration], Phys. Rev. D **92**, 032004 (2015).

[6] CMS Collaboration, CMS-PAS-HIG-14-006.

[7] M. T. Arun and P. Saha, arXiv:1512.06335 [hep-ph]; A. Falkowski and J.F. Kamenik, arXiv:1603.06980 [hep-ph]; C. Csaki and L. Randall, arXiv:1603.07303 [hep-ph]; J. L. Hewett and T.G. Rizzo, arXiv:1603.08250 [hep-ph]; A. Carmona, arXiv:1603.08913 [hep-ph].

[8] K. Hamaguchi and S.P. Liew, arXiv:1604.07828 [hep-ph]; S. Iwamoto *et al.*, arXiv:1604.07776 [hep-ph]; P. Ko, C. Yu and T.C. Yuan, arXiv:1603.08802 [hep-ph]; J.F. Kamenik and M. Redi, arXiv:1603.07719 [hep-ph]; K. Harigaya and Y. Nomura, arXiv:1603.05774 [hep-ph]; Y. Kats and M. Strassler, arXiv:1602.08819 [hep-ph]; Y.J. Zhang, B.B. Zhou and J.J. Sun, arXiv:1602.05539 [hep-ph]; K. Harigaya and Y. Nomura, JHEP **1603**, 091 (2016); J.M. Cline and Z. Liu, arXiv:1512.06827 [hep-ph]; M. x. Luo *et. al.*, Phys. Rev. D **93**, 055042 (2016); C. Han *et al.*, JHEP **1604**, 159 (2016).

[9] M. Drees and M.M. Nojiri, Phys. Rev. Lett. **72**, 2324 (1994); Phys. Rev. D**49**, 4595 (1994); M.J. Herrero, A. Mendez and T.G. Rizzo, Phys. Lett. B**200**, 205 (1988); V.D. Barger and W.Y. Keung, Phys. Lett. B**211**, 355 (1988); B. Batell and S. Jung, JHEP **1507**, 061 (2015); C. Kim *et al.*, Phys. Rev. D**89**, 075010 (2014); S.P. Martin and J.E. Younkin, Phys. Rev. D**80**, 035026 (2009).

[10] S. P. Martin, Phys. Rev. D **77**, 075002 (2008).

[11] J. E. Younkin and S. P. Martin, Phys. Rev. D **81**, 055006 (2010).

[12] G. Aad *et al.* [ATLAS Collaboration], JHEP **1510**, 054 (2015).

[13] V. Khachatryan *et al.* [CMS Collaboration], [arXiv:1602.06581 [hep-ex]].

[14] E. Komatsu *et al.* [WMAP Collaboration], Astrophys. J. Suppl. **192**, 18 (2011).

[15] P. A. R. Ade *et al.* [Planck Collaboration], arXiv:1502.01589 [astro-ph.CO].

[16] P. Huet and A. E. Nelson, Phys. Rev. D **53**, 4578 (1996).

[17] A. Djouadi *et al.*, Comput. Phys. Commun. **176**, 426.

[18] G. Belanger *et al.*, Comput. Phys. Commun. **176**, 367.

[19] N. Baro, F. Boudjema and A. Semenov, Phys. Lett. B **660**, 550 (2008).

[20] D. Asner *et al.*, [HFAG Collaboration], arXiv:1010.1589; M. Misiak *et al.*, Phys. Rev. Lett. **98**, 022002 (2007); J. R. Ellis *et al.*, JHEP **0708**, 083 (2007).

[21] http://indico.cern.ch/getFile.py/access?contribId=4&resId=0&materialId=slides&confId=166286

[22] B. Bhattacherjee *et al.*, Phys. Rev. D **83**, 094026 (2011).

[23] W. Beenakker *et al.*, Nucl. Phys. B **492**, 51 (1997).

[24] P. M. Nadolsky *et al.*, Phys. Rev. D **78**, 013004 (2008).

[25] S. Bornhauser *et al.*, Phys. Rev. D **83**, 035008 (2011).

[26] M. Carena *et al.*, JHEP **0810**, 109 (2008).

[27] M. Drees *et al.*, arXiv:1201.5714 [hep-ph].

[28] G. Aad *et al.* [ATLAS Collaboration], Phys. Rev. D **90**, 052008 (2014).

[29] G. Aad *et al.* [ATLAS Collaboration], JHEP **1409**, 015 (2014).

[30] A. Djouadi, M. M. Muhlleitner and M. Spira, Acta Phys. Polon. B **38**, 635 (2007).

[31] K. Hagiwara *et al.*, Nucl. Phys. B **344**, 1 (1990).

[32] S. Kim, Phys. Rev. D **92**, 094505 (2015).

[33] G. C. Wick, Phys. Rev. **96**, 1124 (1954); R. E. Cutkosky, Phys. Rev. **96**, 1135 (1954).

[34] G.F. Giudice and A. Kusenko, Phys. Lett. B**439**, 55 (1998).

[35] E. Zur Linden and H. Mitter, Nuovo Cim. B **61**, 389 (1969); C. R. Ji and R. J. Furnstahl, Phys. Lett. B **167**, 11 (1986); L. Di Leo and J. W. Darewych, Can. J. Phys. **70**, 412 (1992); T. Nieuwenhuis and J. A. Tjon, Phys. Rev. Lett. **77**, 814 (1996).

[36] J.M. Cornwall *et al.* Phys. Lett. B **718**, 951 (2013).

[37] L. Pearce, A. Kusenko and R. D. Peccei, Phys. Rev. D **88**, 075011 (2013).

[38] M. A. Ajaib, T. Li and Q. Shafi, Phys. Rev. D **85**, 055021 (2012).

[39] B. Kaufman, P. Nath, B. D. Nelson and A. B. Spisak, Phys. Rev. D **92**, 095021 (2015).

[40] The ATLAS collaboration, ATL-PHYS-PUB-2015-053

[41] J. E. Camargo-Molina, B. O'Leary, W. Porod and F. Staub, JHEP **1312**, 103 (2013).

[42] K. Ghosh *et al.*, Phys. Rev. Lett. **110**, 141801 (2013).

[43] G. Aad *et al.* [ATLAS Collaboration], JHEP **1510**, 150 (2015).